A schistosomiasis dataset with bright- and darkfield images

Dieudonné K. Silué [1,2]*, María Díaz de León Derby [3]*, Charles B. Delahunt [4], Anne-Laure Le Ny [4], Ethan Spencer [4], Maxim Armstrong [3], Karla N. Fisher [5,6], Daniel A. Fletcher [3,7,8], Isaac I. Bogoch [5,6,9], Jean T. Coulibaly [1,2]

1 UFR Biosciences, Université Félix Houphouët-Boigny, Abidjan, Côte d'Ivoire.
2 Centre Suisse de Recherches Scientifiques en Côte d'Ivoire, Abidjan Côte d'Ivoire.
3 Department of Bioengineering, University of California, Berkeley, Berkeley, California.
4 Global Health Labs, Inc, Bellevue, Washington.
5 Division of General Internal Medicine, Toronto General Hospital, University Health Network, Toronto, Canada.
6 Division of Infectious Diseases, Toronto General Hospital, University Health Network, Toronto, Canada.
7 Biological Systems and Engineering Division, Lawrence Berkeley National Laboratory, University of California, Berkeley, Berkeley, California.
8 Chan Zuckerberg Biohub, San Francisco, California.
9 Department of Medicine, University of Toronto, Toronto, Canada.
* denotes equal contribution

Correspondence: couljeanvae@yahoo.fr, fletch@berkeley.edu

Abstract
Schistosomiasis is a neglected tropical disease that threatens 700 million and impacts 250 million people per year. The disease is caused by blood flukes of the genus *Schistosoma*, which enter the human body through contact with infected water. One species, *S. haematobium*, sheds eggs through the urinary tract, and can thus be diagnosed by examining urine samples for these eggs. Because concentrations of schistosomiasis infection are highly localized and are often in remote areas, rapid and robust field diagnosis is crucial to both individual diagnosis and the mapping that informs control efforts. AI algorithms, if properly designed, can speed up and improve both diagnosis and mapping through scalable, accurate analysis of images of urine samples. To develop such algorithms, we offer the dataset described here. It consists of paired bright- and darkfield images of urine samples collected in two distinct field studies in Cote d'Ivoire, Africa. There are images from 725 patients, of whom 150 were schisto-positive and contain *S. haematobium* eggs. Crucially, each patient has sufficient images to diagnose *S. haematobium* infection, so the dataset can be used to realistically test the diagnostic value of algorithms for clinical use. The division into two studies allow testing of algorithm generalizability. Due to exigencies of the data collection protocol, the images display a variety of qualities, from clear to blurry, which further allows testing of algorithm robustness to realistic noise. The dataset is thus well-suited to developing algorithms that can be of concrete value in schistosomiasis control efforts.

Keywords
schistosomiasis, Schistosoma haematobium, mobile microscopy, darkfield, machine learning, AI

Article informations

1. Introduction

This paper describes a dataset of images related to schistosomiasis infections, made publicly available for AI researchers to use. A necessary condition for any AI solution to successfully translate to deployment in a clinical setting is that the AI development be, from the start, firmly grounded in and shaped by an understanding of the needs and constraints of the clinical use case. Therefore this Introduction describes the medical specifics of schistosomiasis, its diagnosis, and treatment. Sections 2 and 3 then describe the dataset in detail, and the Discussion contains suggestions as to use of the dataset.

1.1 Schistosomiasis

Schistosomiasis is a worm infection that impacts over 250 million people worldwide, with 90% of the burden on the African continent. The infection is acquired through direct contact to contaminated fresh water, and requires a specific species of snail to complete its lifecyle. The causative pathogen of schistosomiasis is the blood-dwelling trema-

tode of the genus *Schistosoma*. Globally, the most prevalent species are *Schistosoma mansoni* and *S. haematobium*, both living respectively, in the mesenteric and the perivesical venules. The worms lay eggs that are excreted with the feces or urine, and release larvae (miracidia) that infect the suitable intermediate host snails and then mature to a form that can infect humans and complete its life cycle. Schistosomiasis leads to a wide range of clinical presentations ranging from sub-clinical infection to chronic symptoms (i.e., abdominal pain), with additional complications (i.e., periportal fibrosis, bladder cancer, genital ulcerations) and even death. Estimates of the impact of schistosomiasis include 140 million people infected, with 11,500 deaths and over 1.6 million disability-adjusted life years annually (WHO, 2023, 2002; Ogongo et al., 2022; WHO, 2015).

WHO has set an ambitious goal to eliminate schistosomiasis as a public health concern by 2030, calling on all endemic countries to intensify control interventions - mainly mass drug administration using (MDA) praziquantel in entire endemic communities - and strengthen surveillance initiatives (WHO, 2022). Successes in the morbidity control of schistosomiasis based on MDA have been observed in many endemic areas (Japan, China, Egypt etc.) including some sub-Saharan African countries (Utzinger et al., 2009; Rollinson et al., 2013).

1.2 Diagnostics for schistosomiasis

However, a key barrier to elimination of schistosomiasis is lack of a diagnostic tool to cost-effectively target infected individuals when the prevalence become very low, and to monitor MDA programs in areas of high prevalence.

The diagnosis of schistosomiasis in endemic settings is challenging due to the paucity of laboratory resources in lower income rural regions where the majority of infections occur. Diagnosis is typically through direct visualization of the egg, which measures approximately 120 microns (μm), on a stool (*S. mansoni*) or urine (*S. haematobium*) sample. Sample concentration techniques increase the yield of diagnostic testing. The World Health Organization outlines standard laboratory protocols for sample preparation and microscopic diagnosis. Other mechanisms for diagnosis, more commonly performed in higher income areas include serology and molecular techniques.

Given the paucity of laboratory capacity and the extent of infection (and reinfection) in endemic settings, WHO-sanctioned Mass Drug Administration (MDA) programs decrease the burden of schistosomiasis by providing treatment to entire communities in geographic regions where the prevalence of infection is greater than 10%. These programs reduce morbidity and mortality from schistosomiasis, and may be run on an annual or semi-annual basis depending on the community burden of disease. To support this, the WHO has outlined a significant need to monitor MDA programs aimed to control and eliminate schistosomiasis.

The WHO also highlights an urgent need for tools to help monitor and evaluate such MDA programs (World Health Organization Diagnostics Technical Advisory Group (DTAG), 2021). Mapping and diagnosis of schistosomiasis has been done so far with Kato-Katz (KK) and urine filtration (UF), known to be specific but increasingly insensitive as prevalence declines or in low prevalence areas (Colley et al., 2017).

Recently, portable diagnostic tools have shown promising performance in the diagnosis and screening of neglected tropical infections (Vasiman et al., 2019). They may help identifying communities eligible for MDA and other interventions (health education, WASH etc.), and they have attributes that may be useful in monitoring and evaluating schistosomiasis control programs given that they are portable, battery powered, relatively easy to use, and provide a result in real time (Rajchgot et al., 2017).

Handheld digital microscopy is a possible method to evaluate schistosomiasis control programs as such devices are portable so can easily be brought to endemic regions, and are battery powered so do not need to rely on a inconsistent power grids. Such devices are also able to digitize the image, allowing for automated diagnosis.

In this work, we provide a dataset collected on one such device, a portable mobile phone-based microscope called the SchistoScope. This device has been demonstrated as a useful tool for point-of-care diagnosis of *S. haematobium* and other NTDs, such as *Loa loa* (Armstrong et al., 2022; D'Ambrosio et al., 2015; Kamgno et al., 2017).

1.3 Role of AI

Effective AI-driven automated diagnosis is a key approach that can provide breakthroughs to improving the efficiency of screening, because it can overcome the challenges of a paucity of trained microbiologists and laboratory personnel. However, schistosomiasis diagnostics are currently gravely underserved by the medical AI community. The purpose of this dataset is to enable development of AI solutions that can meet the stringent clinical requirements of this use case. In particular, the dataset enables development and evaluation of models (i) at the patient-level (since it has 725 patients); (ii) on true holdout sets (since two studies are represented); and (iii) for robustness to blur noise.

2. Dataset acquisition details

This section describes how the dataset was collected.

2.1 Sample collection

Ethical permission for this study was granted by Comité National d'Ethique des Sciences de la Vie et de la Santé (CNESVS) in Côte d'Ivoire and the University Health Network, Toronto, Canada (REB 186-21/MSHPCMU/CNESVS-km)). Permission was also granted by the local Health District officer. School-age children between 6 and 15 years were invited to participate, and both signed parental consent and the children's assent were required for inclusion.

Sample processing and dataset collection happened during two visits to the Azaguié region in Côte d'Ivoire: A first visit in March of 2020, described in Coulibaly et al. (2023); and a second visit in November of 2021, described in Coulibaly et al. (2024).

Patient sample processing is described in (Armstrong et al., 2022). Briefly, for each patient, 10 mL of urine were collected in a sterile urine container between the hours of 10 am - 2 pm. The cup was shaken and 10mL of urine was removed by a syringe and pressed through a plastic capillary designed to concentrate *S. haematobium* eggs. The capillaries were designed to capture objects that are the size of *S. haematobium* eggs by having a channel that is 3 mm wide and a height that decreases from 200 μm to a 20 μm pinchpoint over a 30 mm length. The capillaries have an inlet, where the disposable syringe is connected, and a circular outlet port that allows excess urine to exit. In the field, the eggs, as well as other debris found in the patient urine samples, are trapped in the capillaries as the urine solution flows through. The capillaries help to concentrate the sample and are simultaneously used for imaging the sample contents using a handheld digital microscope.

2.2 Image acquisition

The images for both datasets were acquired using the SchistoScope, a portable, mobile phone-based microscope described in Armstrong et al. (2022). Briefly, this device uses an Apple iPhone 8 coupled to an additional reversed lens to capture images with a large field of view (FoV) and $< 5\ \mu m$ resolution over a 12-mm^2 area. The SchistoScope uses two sets of LEDs for illumination, allowing for multi-contrast image acquisition:
(i) Brightfield: A set of LEDs positioned directly below the sample enables brightfield imaging.
(ii) Darkfield: An additional set of LEDs is positioned to the side, in a configuration such that the light hits the sample but does not directly hit the imaging lens. In this darkfield illumination, objects trapped in the capillary scatter the illumination light, and only the scattered light is collected by the imaging lens. This creates images with bright objects and a dark background. Field clinicians report that darkfield is a valuable modality for manual assessment. For example images, see Fig 2.

After sample preparation, the capillaries with the patient sample are inserted into the SchistoScope for image acquisition using both the brightfield and darkfield contrasts. The capillaries are physically translated using a servomotor along their horizontal axis so that multiple locations can be imaged. Six fields of view of the capillaries were imaged using brightfield and darkfield illumination.

3. Dataset contents

This section details the structure and contents of the dataset.

3.1 Structure

The dataset is structured as follows. There are image sets from two different field studies, conducted in March 2020 and November 2021. The March 2020 dataset has 349 patients, 91 of whom are positive. The November 2021 dataset has 376 patients, 59 of whom are positive. Each patient has 3 slightly overlapping fields of view (FoVs), captured with both brightfield and darkfield, giving 6 images per patient.

3.2 Egg locations and FoV details

Due to the design and flow direction of the capillaries, most *S. haematobium* eggs and debris are found near the pinchpoint and the outlet port (since some eggs get past the pinchpoint). These crucial regions are captured within the final 3 FoVs. In high parasitemia patients, eggs are occasionally found in the FoV immediately upstream from the pinchpoint. The other 4 upstream FoVs are empty. Therefore the dataset includes 3 FoVs per patient.

We note that the device alignment shifted slightly between the two studies, resulting in a change as to which FoVs contain the most eggs: (i) In March 2020, most eggs were trapped in FoVs 1 and 2 (which in this study corresponded to outlet port and pinchpoint), with occasional eggs in the 3rd FoV; (ii) In November 2021, FoVs 2 and 3 contain the outlet hole and pinchpoint and thus almost all the eggs, while image 1 is downstream from the outlet port and thus generally empty. Example patients showing these FoV layouts are given in Fig 1.

The provided images are 4032 $\times$ 3024 pixels, with pixel pitch $\approx 1\ \mu m$/pixel. The optical resolution of the SchistoScope is estimated to be $< 5\ \mu m$ (Armstrong et al., 2022) and the images can be downsampled 2$\times$ or even 3-4$\times$ An example of brightfield and darkfield images of a FoV are shown in the top part of Figure 2. The *S. haematobium* egg locations in those images are then highlighted by green boxes in the bottom part of Figure 2. Zoomed-in examples of *S. haematobium* eggs and distractor objects are shown in Figure 3.

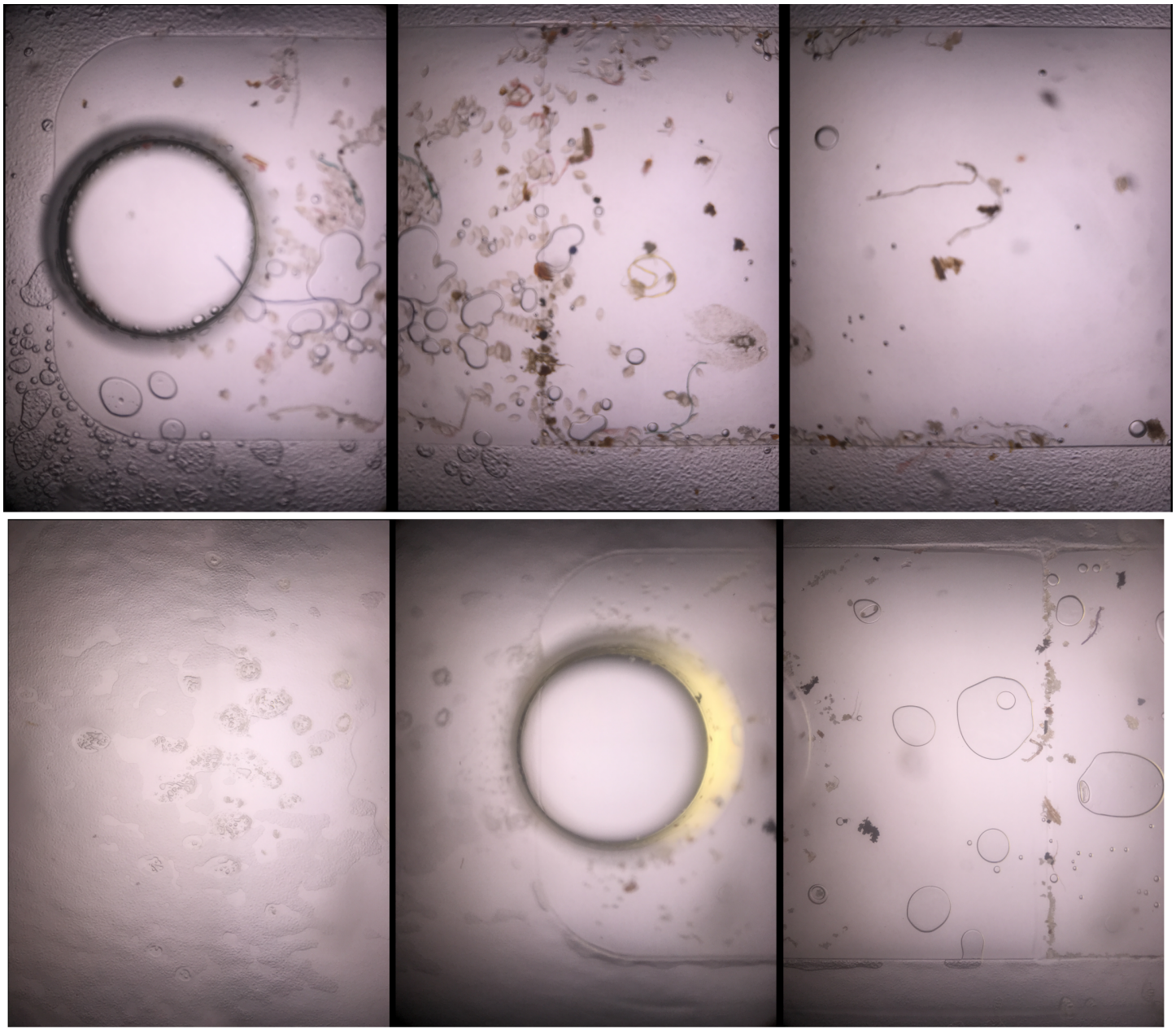

Figure 1: Three brightfield FoVs, showing outlet port and pinchpoint. Top: March 2020. Bottom: November 2021. The degree of overlap can be inferred from landmark features. The overwhelming majority of eggs are in FoVs 1 and 2 (for March 2020) and FoVs 2 and 3 (for November 2021).

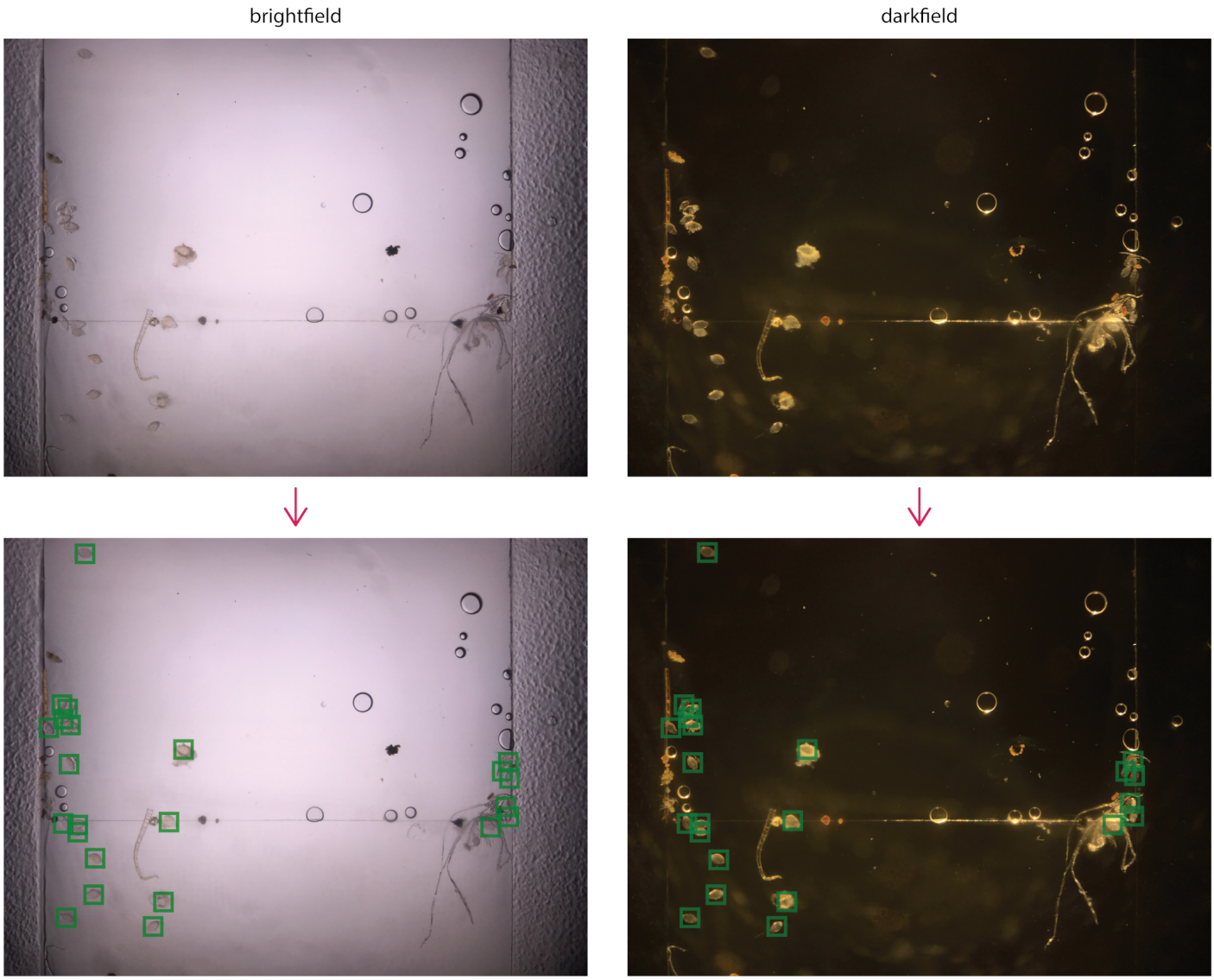

Figure 2: Example images of a FoV in brightfield and darkfield (top) and the corresponding *S. haematobium* egg annotations

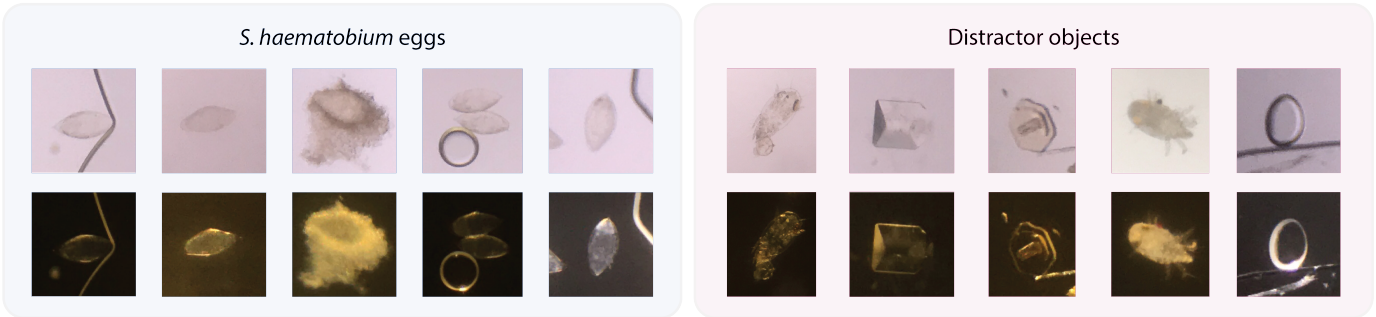

Figure 3: Examples of *S. haematobium* eggs and distractor objects found in the brightfield and darkfield dataset images.

3.2.1 Quality

Due to the experimental nature of the capillaries and device, field testing uncovered a tendency towards images blurred by stray droplets or smears of water or urine on parts of the capillary window and/or device optics.

For the same FoV, BF and DF images can have different blur characterists due to optical effects. Sometimes a single image has different subregions that are blurred and in focus. Statistics for blur prevalence are given in 3.4.

3.3 Annotations

There are two types of annotations: object-level *S. haematobium* egg (as well as "doubtful" object) locations, and image-level quality labels.

Egg locations All of the images were reviewed by two annotators that were trained to identify *S. haematobium* eggs. The first annotator examined all images and labeled *S. haematobium* eggs and "doubtful objects". After this first pass, the second annotator went through the images to revise the annotations and mark any *S. haematobium* eggs that the first annotator missed. A third annotator was consulted in cases of disagreement.

"Doubtfuls" are objects that look similar to an egg, such that the annotators could not definitively label them as eggs or as non-eggs. This uncertainty makes them objects of particular interest, which require special care during ML model training and assessment.

Distractor objects are not annotated. We strove to completely annotate eggs and doubtful objects, so any unlabeled object can be (we hope) considered a distractor.

The annotations for the entire dataset are provided in a spreadsheet format, one for each study. For each annotation, the spreadsheet contains information on the patient ID, parent image name, object label (egg or doubtful), and (x,y) coordinates of the centre of the object.

Because the brightfield and darkfield images of an FoV almost exactly match spatially, the (x, y) coordinates of eggs in paired images are typically within a few pixels of each other. However, in some cases an object is doubtful in one contrast but not the other, or not visible in one of the contrasts due to blur. In these cases the annotations of paired images do not match.

Quality labels The images of the March 2020 dataset were also given an approximate quality score by one annotator. All of the images in the dataset are given a score from 0-12, where a lower score corresponds to an image of better quality. The quality rating meanings are given in Table 3.3.

The three main aspects of imperfect quality are: blurriness (due to failures of the SchistoScope autofocus mechanism), haziness (due to evaporation of urine or other liquid), and wetness (due to the presence of urine or other liquid on the capillaries). These three categories are represented in the quality annotations provided in a spreadsheet format. Since the autofocus routine was run separately when acquiring brightfield and darkfield images, and since the contrasts have optical properties, brightfield and darkfield images of the same field-of-view often have different quality scores (see 3.4).

Table 1: Quality ratings for image blurriness. These ratings roughly group into 4 categories: 0 - 1 excellent; 2 - 4 medium-high; 5 - 7 medium; 8 - 12 lowest.

0	perfect	2	little blurry
1	almost perfect	3	little hazy
		4	little wet
5	blurry	8	blurry and hazy
6	hazy	9	blurry and wet
7	wet	10	hazy and wet
		11	dirty, other
		12	hazy, blurry, and wet

3.4 Dataset statistics

This section provides patient-level egg count statistics for each study, and also image-level quality statistics for March 2020.

Egg counts March 2020 had 258 negative and 91 positive patients, with a total of 2999 labeled eggs and 308 labeled doubtfuls. November 2021 had 317 negative and 59 positive patients, with a total of 2478 labeled eggs and 449 doubtfuls. Patient-level count distributions for each study are given in Fig 4 (A and B). Most of the patients have light intensity infections (WHO, 2002). Note that these are *not* per-FoV counts, because the clinically-relevant unit is the patient, not the FoV (or image, or image patch). Many FoVs contain no eggs, especially in low parasitemia patients.

Quality The per-image quality (i.e. blurriness) distributions for brightfield and darkfield images in the March 2020 study are shown in Fig 5 (A and B). Because bright field and dark field images were affected in different ways by blur, even in the same FoV, each contrast has different histograms. These quality differences between paired images (brightfield-darkfield) are scatterplotted in Fig 5 (C).

3.5 Data location and availability

The dataset was structured according to FAIR principles (Wilkinson et al., 2016). It will be hosted on and freely available from the AFRICAI Repository at the Euro-Bio-

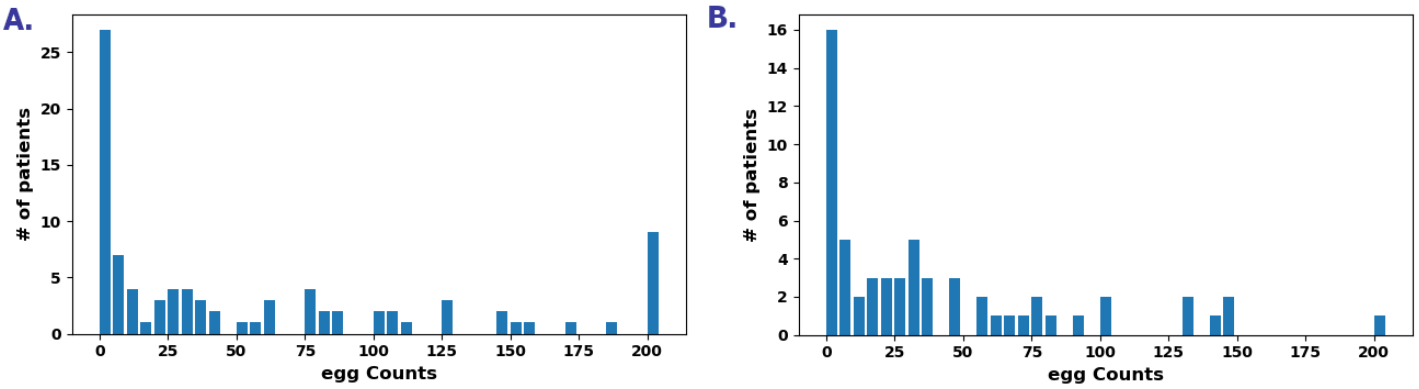

Figure 4: Histograms of egg counts by patient, binned by 5's (i.e. 1-5, 6-10, etc). A: March 2020, 91 positive patients. B: November 2021, 59 positive patients.

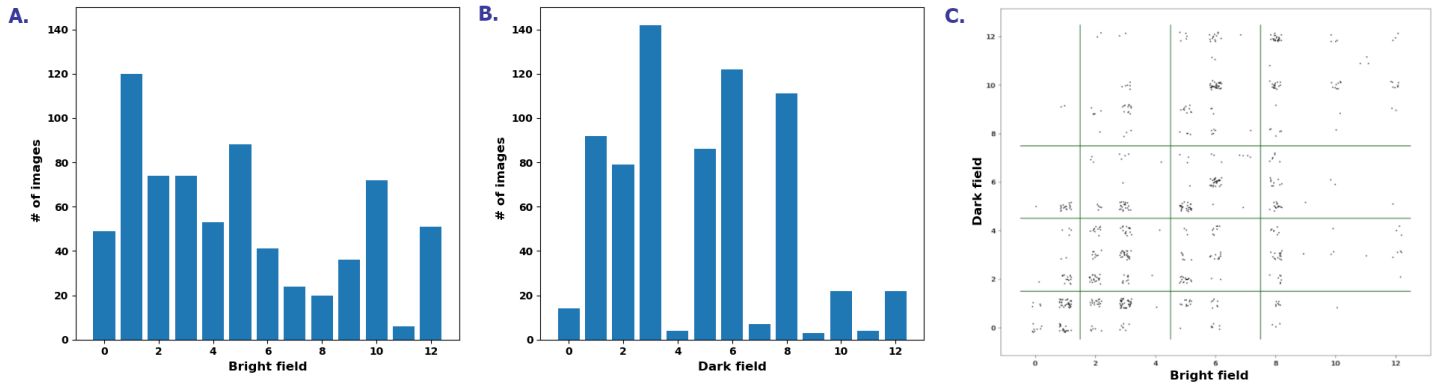

Figure 5: Histogram of March 2020 image qualities. A: Bright field. B: Dark field. C: Scatterplot of dark field vs bright field image qualities (each point is an FoV; the points are jittered to show quantities). The same FoV often has different image quality in the two contrasts.

Imaging Medical Imaging Archive XNAT (Martijn and Tsirikoglo, 2024).
Note to reviewers: Pending initial acceptance, we will upload the data to the repo before final acceptance (≈ mid-August). At that point we will insert exact download details here.

4. Discussion

AI can certainly have vast impact for good in the diagnosis of schistosomiasis. However, for any AI model to successfully translate to the clinic, and thus benefit sick people, it is crucial that the AI development be firmly grounded in and tailored to the particular needs of the clinical use case. For example, metrics to evaluate a model's performance should reflect the role it will serve as part of a clinical solution, as opposed to based on generic performance metrics imported from the AI literature. For a detailed discussion of how to select metrics to guide AI development, given for automated malaria diagnosis with applicability to schistosomiasis, see Delahunt et al. (2024).

Crucially, when proposing solutions in medical applications, the rules of evidence are determined by medical norms, not by AI standards and conventions. See WHO's document on the types of evidence required to validate AI models for medical use cases (WHO, 2021). See also discussions of AI metrics in Reinke and Tizabi (2024) and (Varoquaux and Cheplygina, 2022).

The dataset described here is well-suited for AI efforts to realistically address the problem of schistosomiasis diagnosis. In particular, development and evaluation can operate at the patient level, the two studies enable true holdout evaluation, and the blurring effects enable development and evaluation for robustness to the realistic case of lower quality images. Despite the stringent performance requirements in the WHO TPP (World Health Organization Diagnostics Technical Advisory Group (DTAG), 2021) (e.g., 97.5% specificity and 85% sensitivity even at very low parasitemias), we are confident that AI models, if developed with proper attention to the specific clinical needs, will have powerful impact in reducing the damage from this neglected tropical disease.

Acknowledgments

DAF acknowledges support from the Harvey and Leslie Wagner Foundation and a gift from Mitz and Lucinda Igarashi. IIB is supported by the Canadian Institutes of Health Research (PJT-83575).

Ethical Standards

Ethical permission for this study was granted by Comité National d'Ethique des Sciences de la Vie et de la Santé (CNESVS) in Côte d'Ivoire and the University Health Network, Toronto, Canada (REB 186-21/MSHPCMU/CNESVS-km)). Permission was also granted by the local Health District officer. School-age children between 6 and 15 years were invited to participate, and both signed parental consent and the children's assent were required for inclusion.

Conflicts of Interest

IIB consults to the Weapons Threat Reduction Program at Global Affairs Canada. The other authors declare that we don't have conflicts of interest.

References

M. Armstrong, A.R. Harris, M.V. D'Ambrosio, J.T. Coulibaly, S. Essien-Baidoo, R.K.D. Ephraim, J.R. Andrews, I.I. Bogoch, and D.A. Fletcher. Point-of-care sample preparation and automated quantitative detection of Schistosoma haematobium using mobile phone microscopy. *Am J Trop Med Hyg*, 2022. URL https://www.ajtmh.org/view/journals/tpmd/106/5/article-p1442.xml.

D.G. Colley, T.S. Andros, and C.H. Campbell. Schistosomiasis is more prevalent than previously thought: what does it mean for public health goals, policies, strategies, guidelines and intervention programs? *Infectious Diseases of Poverty*, 2017. URL 10.1186/s40249-017-0275-5.

J.T. Coulibaly, K.D. Silue, M. Armstrong, M. Díaz de León Derby, M.V. D'Ambrosio, D.A. Fletcher, J. Keiser, K. Fisher, J.R. Andrews, and I.I. Bogoch. High sensitivity of mobile phone microscopy screening for Schistosoma haematobium in Azaguié, Côte d'Ivoire. *Am J Trop Med Hyg*, 2023. URL https://www.ajtmh.org/view/journals/tpmd/108/1/article-p41.xml.

J.T. Coulibaly, K.D. Silue, M. Díaz de León Derby, D.A. Fletcher, K.N. Fisher, J.R. Andrews, and I.I. Bogoch. Rapid and comprehensive screening for urogenital and gastrointestinal schistosomiasis with handheld digital microscopy combined with circulating cathodic antigen testing. *Am J Trop Med Hyg*, 2024. URL 10.4269/ajtmh.24-0043.

C.B. Delahunt, N. Gachuhi, and M.P Horning. Metrics

to guide development of machine learning algorithms for malaria diagnosis. *Frontiers Malaria*, 2024. URL https://doi.org/10.3389/fmala.2024.1250220.

M.V. D'Ambrosio, M. Bakalar, S. Bennuru, C. Reber, A. Skandarajah, L. Nilsson, N. Switz, J. Kamgno, S. Pion, M. Boussinesq, T.B. Nutman, and D.A. Fletcher. Point-of-care quantification of blood-borne filarial parasites with a mobile phone microscope. *Science Translational Medicine*, 2015. URL https://www.science.org/doi/abs/10.1126/scitranslmed.aaa3480.

J. Kamgno, S.D. Pion, C.B. Chesnais, M.H. Matthew H. Bakalar, M.V. D'Ambrosio, C.D. Mackenzie, H.C. Nana-Djeunga, Raceline Gounoue-Kamkumo, G.-R. Njitchouang, P. Nwane, J.B. Tchatchueng-Mbouga, S. Wanji, W.A. Stolk, D.A. Fletcher, A.D. Klion, T.B. Nutman, and M. Boussinesq. A test-and-not-treat strategy for onchocerciasis in loa loa-endemic areas. *New England J Medicine*, 2017. URL https://www.nejm.org/doi/full/10.1056/NEJMoa1705026.

P.A. Martijn and A. Tsirikoglo. AFRICAI Imaging Repository White Paper. *MICCAI*, 2024. URL https://zenodo.org/doi/10.5281/zenodo.10816768.

P. Ogongo, R.K. Nyakundi, G.K. Chege, and L. Ochola. The road to elimination: Current state of schistosomiasis research and progress towards the end game. *Frontiers in Immunology*, 2022. URL 10.3389/fimmu.2022.846108.

J. Rajchgot, J.T. Coulibaly, J. Keiser, J. Utzinger, N.C. Lo, M.K. Mondry, J.R. Andrews, and I.I. Bogoch. Mobile-phone and handheld microscopy for neglected tropical diseases. *PLoS Negl. Trop. Dis.*, 2017.

A. Reinke and M.D. et al. Tizabi. Understanding metric-related pitfalls in image analysis validation. *Nature Methods*, 2024. URL https://doi.org/10.1038/s41592-023-02150-0.

D. Rollinson, S. Knopp, S. Levitz, J.R. Stothard, L.-A. Tchuem Tchuenté, A. Garba, K.A. Mohammed, N. Schur, B. Person, D.G. Colley, and J. Utzinger. Time to set the agenda for schistosomiasis elimination. *Acta Tropica*, 2013. URL https://doi.org/10.1016/j.actatropica.2012.04.013.

J. Utzinger, G. Raso, S. Brooker, D. de Savigny, M. Tanner, N. Ørnbjerg, B.H. Singer, and E.K. N'Goran. Schistosomiasis and neglected tropical diseases: towards integrated and sustainable control and a word of caution. *Parasitology*, 2009. URL 10.1017/S0031182009991600.

G. Varoquaux and V. Cheplygina. Machine learning for medical imaging: methodological failures and recommendations for the future. *npj Digital Medicine*, 2022. URL https://doi.org/10.1038/s41746-022-00592-y.

A. Vasiman, J.R. Stothard, and I.I. Bogoch. Mobile phone devices and handheld microscopes as diagnostic platforms for malaria and neglected tropical diseases (NTDs) in low-resource settings: A systematic review, historical perspective and future outlook. In J. Keiser, editor, *Highlighting Operational and Implementation Research for Control of Helminthiasis*, Advances in Parasitology. Academic Press, 2019. URL https://doi.org/10.1016/bs.apar.2018.09.001.

WHO. *Prevention and control of schistosomiasis and soil-transmitted helminthiasis*, 2002. World Health Organization, Geneva, Switzerland.

WHO. *Female genital schistosomiasis: A pocket atlas for clinical health-care professionals*, 2015. World Health Organization, Geneva, Switzerland.

WHO. *Generating evidence for artificial intelligence-based medical devices: a framework for training, validation and evaluation*, 2021. World Health Organization, Geneva, Switzerland.

WHO. *WHO guideline on control and elimination of human schistosomiasis*, 2022. World Health Organization, Geneva, Switzerland.

WHO. *Global report on neglected tropical diseases 2023*, 2023. World Health Organization, Geneva, Switzerland.

M.D. Wilkinson, B. Mons, and et al. The FAIR Guiding Principles for scientific data management and stewardship. *Scientific Data*, 2016. URL https://doi.org/10.1038/sdata.2016.18.

World Health Organization Diagnostics Technical Advisory Group (DTAG). Diagnostic target product profiles for monitoring, evaluation and surveillance of schistosomiasis control programmes. https://www.who.int/publications/i/item/9789240031104, 2021. Accessed: 10.16.2023.